PHYSICAL REVIEW D **92,** 024037 (2015)

Stellar models in brane worlds

Francisco X. Linares,[1,2,*] Miguel A. García-Aspeitia,[3,4,†] and L. Arturo Ureña-López[1,5,‡]

[1]*Departamento de Física, DCI, Campus León, Universidad de Guanajuato, Código Postal 37150, León, Guanajuato, México*

[2]*Departamento de Física, Universidad Simón Bolívar Apartado 89000, Caracas 1080A, Venezuela*

[3]*Consejo Nacional de Ciencia y Tecnología, Avenida Insurgentes Sur 1582, Colonia Crédito Constructor, Delegación Benito Juárez, Código Postal 03940, México Distrito Federal, México*

[4]*Unidad Académica de Física, Universidad Autónoma de Zacatecas, Calzada Solidaridad esquina con Paseo a la Bufa S/N, Código Postal 98060, Zacatecas, México*

[5]*Institute for Astronomy, University of Edinburgh, Royal Observatory, Edinburgh EH9 3HJ, United Kingdom*

(Received 23 January 2015; published 20 July 2015)

We consider here a full study of stellar dynamics from the brane-world point of view in the case of constant density and of a polytropic fluid. We start our study cataloguing the minimal requirements to obtain a compact object with a Schwarzschild exterior, highlighting the low and high energy limit, the boundary conditions, and the appropriate behavior of Weyl contributions inside and outside of the star. Under the previous requirements we show an extensive study of stellar behavior, starting with stars of constant density and its extended cases with the presence of nonlocal contributions. Finally, we focus our attention to more realistic stars with a polytropic equation of state, especially in the case of white dwarfs, and study their static configurations numerically. One of the main results is that the inclusion of the Weyl functions from brane-world models allows the existence of more compact configurations than within general relativity.

DOI: 10.1103/PhysRevD.92.024037 PACS numbers: 04.50.-h, 04.40.Dg

I. INTRODUCTION

Stellar astrophysics is one of the most characteristic topics studied by general relativity (GR), which has helped to describe the dynamic and evolution of stars with unprecedented success [1]. In addition, the matter inside a star may be in some cases in extreme conditions generating complicated high energy phenomena, principally in white dwarfs, neutron stars, and others, and then a complete description of the stellar properties requires the introduction of a particular equation of state (EOS) like in the case of polytropes [2], or even Bose-Einstein condensates [3].

Another interesting possibility in recent times is to consider alternative theories of gravity and to look for their particular signatures in stellar models, especially for some of the extreme situations mentioned above. For instance, the authors in [4] considered the corrections induced by a Galileon Lagrangian in stars of constant density. Another example is given by the so-called models of brane worlds (see [5,6] for a good review) whose main characteristic is the existence of branes (four-dimensional manifolds) embedded in a five-dimensional bulk, the known Randall-Sundrum (RS) models [7]. This particular geometry allows a natural extension of Einstein's equations [8], and introduces new degrees of freedom through quadratic terms of the energy-momentum tensor, the nonlocal Weyl terms, and other fields that could live in the bulk. This framework has been used for stars with a constant density in [9], and also for polytropic matter with a given relationship between the quantities arising from the nonlocal Weyl terms in [10]. It has also been shown that the exterior solution of these brane stars is not the Schwarzschild one [9,11], and then the Weyl fluids in the exterior of the stars can have a non-negligible influence in the internal pressure and compactness of stellar objects. More recently, the conditions for stellar stability in brane stars were revisited in [12] for a set of hypotheses called the *minimal setup*, which are consistent with a Schwarzschild exterior. Also, see [13] for a study on the gravitational collapse of brane stars.

We would like to mention here some experimental constraints on brane-world models, most of them about the so-called brane tension λ, which appears explicitly as a free parameter in the corrections of the gravitational equations mentioned above. As a first example we have the measurements on the deviations from Newton's law of the gravitational interaction at small distances. It is reported that no deviation is observed for distances $l \gtrsim 0.1$ mm, which then implies a lower limit on the brane tension in the model Randall-Sundrum II: $\lambda > 1$ TeV^4 [14]; it is important to mention that these limits do not apply to the two-branes case of the model Randall-Sundrum I (see [6] for details). Astrophysical studies related with gravitational

*linares.francisco@gmail.com
†aspeitia@fisica.uaz.edu.mx
‡lurena@fisica.ugto.mx

waves and stellar stability constrain the brane tension as $\lambda > 5 \times 10^8$ MeV^4 [9,15], whereas the existence of black hole x-ray binaries suggest that $l \lesssim 10^{-2}$ mm [6,16]. Finally, from cosmological observations, the requirement of successful nucleosynthesis provides the lower limit $\lambda > 1$ MeV^4, which is a much weaker limit as compared to other experiments (other cosmological tests can be seen in [17]).

With the previous background, this paper is dedicated to the study of the stellar equations of motion that arise from the formalism of brane-world theory, and the role of the Weyl functions in the regular behavior of a stellar distribution. It is important to remark that our main objective is to consider models of stars as realistic as possible, and for this reason we will follow conventional wisdom in this regard: a Schwarzschild exterior, and regularity of all functions involved. Based on these premises, we perform numerical studies of the so-called extended Germani-Maartens (GM) solution with constant density, and of a polytropic fluid.

The organization of the paper is as follows. In Sec. II, we describe the equations of stellar dynamics with branes, emphasizing the high and low energy limits, boundary conditions, and the role played by the Weyl functions in providing consistent and regular solutions. Subsequently, in Sec. III, we study the case of constant density and the extended GM solution. Also, in Sec. IV we study polytropic brane stars. Finally, in Sec. V we give some conclusions and remarks.

II. STELLAR DYNAMICS WITH BRANES

Let us start by writing the equations of motion for an embedded brane in a five-dimensional bulk using the RS II model [7]. We first assume that the Einstein equations are the gravitational equations of motion of the five-dimensional universe,

$$G_{AB} + \Lambda_{(5)} g_{AB} = \kappa^2_{(5)} T_{AB}. \tag{1}$$

Following an appropriate computation, the modified four-dimensional Einstein's equation can be written as [6,8]

$$G_{\mu\nu} + \xi_{\mu\nu} + \Lambda_{(4)} g_{\mu\nu} = \kappa^2_{(4)} T_{\mu\nu} + \kappa^4_{(5)} \Pi_{\mu\nu} + \kappa^2_{(5)} F_{\mu\nu}, \tag{2}$$

where $\kappa_{(4)}$ and $\kappa_{(5)}$ are, respectively, the four- and five-dimensional coupling constants, which are related to each other in the form: $\kappa^2_{(4)} = 8\pi G_N = \kappa^4_{(5)}\lambda/6$, λ is defined as the brane tension, and G_N is Newton's constant. For purposes of simplicity, we will not consider bulk matter, which translates into $F_{\mu\nu} = 0$, and discard the presence of the four-dimensional cosmological constant, $\Lambda_{(4)} = 0$, as we do not expect it to have any important effect at astrophysical scales (for a recent discussion about it see [18]). Additionally, we will neglect any nonlocal energy flux, which is allowed by the static spherically symmetric solutions we will study below [6].

In the case of a perfect fluid, the energy-momentum $T_{\mu\nu}$ tensor, the quadratic energy-momentum tensor $\Pi_{\mu\nu}$, and the Weyl $\xi_{\mu\nu}$ can be written as

$$T_{\mu\nu} = \rho u_\mu u_\nu + p h_{\mu\nu}, \tag{3a}$$

$$\Pi_{\mu\nu} = \frac{1}{12}\rho[\rho u_\mu u_\nu + (\rho + 2p) h_{\mu\nu}], \tag{3b}$$

$$\xi_{\mu\nu} = -\frac{6}{\kappa^2_{(4)}\lambda}\left[\mathcal{U} u_\mu u_\nu + \mathcal{P} r_\mu r_\nu + \frac{\mathcal{U} - \mathcal{P}}{3} h_{\mu\nu}\right], \tag{3c}$$

where $p = p(r)$ and $\rho = \rho(r)$ are, respectively, the pressure and density of the stellar matter of interest, $\mathcal{U}$ is the nonlocal energy density, $\mathcal{P}$ is the nonlocal anisotropic stress scalar, u_α is the fluid four-velocity, which also satisfies the condition $g_{\mu\nu}u^\mu u^\nu = -1$, and $h_{\mu\nu} = g_{\mu\nu} + u_\mu u_\nu$ is orthogonal to u_μ. Under the assumption of spherical symmetry, the metric can be written as

$$ds^2 = -B(r)dt^2 + A(r)dr^2 + r^2(d\theta^2 + \sin^2\theta d\varphi^2). \tag{4}$$

The equations of motion for stellar structure then are [9,12]

$$\mathcal{M}' = 4\pi r^2 \rho_{\text{eff}}, \tag{5a}$$

$$p' = -\frac{1}{2}\frac{B'}{B}(p + \rho), \tag{5b}$$

$$\mathcal{V}' + 3\mathcal{N}' = -\frac{B'}{B}(2\mathcal{V} + 3\mathcal{N}) - \frac{9}{r}\mathcal{N} - 3(\rho + p)\rho', \tag{5c}$$

$$\frac{B'}{B} = \frac{2G_N}{r^2}\left(\frac{4\pi r^3 p_{\text{eff}} + \mathcal{M}}{1 - 2G_N\mathcal{M}/r}\right), \tag{5d}$$

where a prime indicates derivative with respect to r. We have also defined $\mathcal{V} = 6\mathcal{U}/\kappa^4_{(4)}$, $\mathcal{N} = 4\mathcal{P}/\kappa^4_{(4)}$, and $A(r) = [1 - 2G_N\mathcal{M}(r)/r]^{-1}$, whereas p_{eff} and ρ_{eff} are explicitly given by

$$p_{\text{eff}} = p\left(1 + \frac{\rho}{\lambda}\right) + \frac{\rho^2}{2\lambda} + \frac{\mathcal{V}}{3\lambda} + \frac{\mathcal{N}}{\lambda}, \tag{6a}$$

$$\rho_{\text{eff}} = \rho\left(1 + \frac{\rho}{2\lambda}\right) + \frac{\mathcal{V}}{\lambda}. \tag{6b}$$

Now, we are in position to analyze the following important points.

A. Numerical analysis

In order to have a numerical solution of the equations of motion, we choose the following dimensionless variables:

$$x = \sqrt{G_N M/R}(r/R), \quad \bar{\rho} = \rho/\langle\rho_{\text{eff}}\rangle, \quad \bar{p} = p/\langle\rho_{\text{eff}}\rangle, \tag{7a}$$

$$\bar{\lambda}=\lambda/\langle\rho_{\rm eff}\rangle,\quad \bar{\mathcal{V}}=\mathcal{V}/\langle\rho_{\rm eff}\rangle^2,\quad \bar{\mathcal{N}}=\mathcal{N}/\langle\rho_{\rm eff}\rangle^2, \tag{7b}$$

for which Eq. (5) reads

$$\bar{\mathcal{M}}' = x^2\bar{\rho}_{\rm eff}, \tag{8a}$$

$$\bar{p}' = -\frac{3}{x^2}\left(\frac{x^3\bar{p}_{\rm eff}+\bar{\mathcal{M}}}{1-6\bar{\mathcal{M}}/x}\right)(\bar{p}+\bar{\rho}), \tag{8b}$$

$$\bar{\mathcal{V}}'+3\bar{\mathcal{N}}' = -\frac{6}{x^2}\left(\frac{x^3\bar{p}_{\rm eff}+\bar{\mathcal{M}}}{1-6\bar{\mathcal{M}}/x}\right)(2\bar{\mathcal{V}}+3\bar{\mathcal{N}}) - \frac{9}{x}\bar{\mathcal{N}} - 3(\bar{p}+\bar{p})\bar{\rho}', \tag{8c}$$

where now a prime denotes derivatives with respect to x, the mean effective density is just given by $\langle\rho_{\rm eff}\rangle = 3M/4\pi R^3$, and also

$$\bar{\rho}_{\rm eff} = \bar{\rho}\left(1+\frac{\bar{\rho}}{2\bar{\lambda}}\right)+\frac{\bar{\mathcal{V}}}{\bar{\lambda}}, \tag{9a}$$

$$\bar{p}_{\rm eff} = \bar{p}\left(1+\frac{\bar{\rho}}{\bar{\lambda}}\right)+\frac{\bar{\rho}^2}{2\bar{\lambda}}+\frac{\bar{\mathcal{V}}}{3\bar{\lambda}}+\frac{\bar{\mathcal{N}}}{\bar{\lambda}}. \tag{9b}$$

Note that the ratio ρ/λ is invariant under the change of variables, $\bar{\rho}/\bar{\lambda}=\rho/\lambda$, and then we will omit the bar whenever the ratio appears in the equations of motion.

B. High and low energy limits

There are two very clear limiting expressions of the equations of motion in terms of normalized brane ratio $\bar{\lambda}$, as the latter represents the energy ratio of the brane tension with respect to the mean energy density of the compact star of interest; see Eq. (7b). It is usually assumed that the brane corrections are measured in terms of the absolute value of the brane tension λ, but in our study we find the brane ratio $\bar{\lambda}=\lambda/\langle\rho_{\rm eff}\rangle$ to have a more meaningful character for compact objects in general.

Under this line of reasoning, we first present the low energy limit of the equations of motion, represented by the operation $\bar{\lambda}\to\infty$, under which Eqs. (8a)–(8c) become the usual Tolman-Oppenheimer-Volkoff (TOV) equations of GR [1,2]:

$$\bar{\mathcal{M}}' = x^2\bar{\rho}, \tag{10a}$$

$$\bar{p}' = -\frac{3}{x^2}\left(\frac{x^3\bar{p}+\bar{\mathcal{M}}}{1-6\bar{\mathcal{M}}/x}\right)(\bar{p}+\bar{\rho}), \tag{10b}$$

where the effective pressure and density are directly represented by their normalized physical values.We have called it the low energy limit because we are assuming that the mean density of the star is much lower than the brane tension λ, so that any brane corrections in the equations of motion are highly suppressed by the brane energy scale. We cannot say here whether the brane tension is at a very high energy scale, or if it is just that the star density is not high enough. In the strict sense, Eq. (8c) can still be considered for the integration of the Weyl functions, but their values will not make any difference in the final integration of the physical variables.

There is also the high energy limit of the equations of motion represented by $\bar{\lambda}\to 0$, for which the effective density and pressure read

$$\bar{\rho}_{\rm eff} \simeq \frac{\bar{\rho}^2}{2\bar{\lambda}}+\frac{\bar{\mathcal{V}}}{\bar{\lambda}}, \tag{11a}$$

$$\bar{p}_{\rm eff} \simeq \frac{\rho}{2\lambda}(2\bar{p}+\bar{\rho})+\frac{\bar{\mathcal{V}}}{3\bar{\lambda}}+\frac{\bar{\mathcal{N}}}{\bar{\lambda}}. \tag{11b}$$

We can see that there is an overall factor of $\bar{\lambda}$ in the above expressions (11), which will also appear as such in Eq. (8) in the high energy limit. The brane ratio can then be absorbed in the equations of motion by means of the following change of variables: $\bar{\mathcal{M}}\to\bar{\mathcal{M}}\bar{\lambda}^{1/2}$, and $x\to x\bar{\lambda}^{1/2}$, and then we finally find the equations of motion for the high energy limit:

$$\bar{\mathcal{M}}' = \frac{x^2}{2}(\bar{\rho}^2+2\bar{\mathcal{V}}), \tag{12a}$$

$$\bar{p}' = -\frac{3}{x^2}\left[\frac{x^3(\bar{p}\,\bar{\rho}+\bar{\rho}^2/2+\bar{\mathcal{V}}/3+\bar{\mathcal{N}})+\bar{\mathcal{M}}}{1-6\bar{\mathcal{M}}/x}\right](\bar{p}+\bar{\rho}), \tag{12b}$$

$$\bar{\mathcal{V}}'+3\bar{\mathcal{N}}' = -\frac{6}{x^2}\left(\frac{x^3(\bar{p}\,\bar{\rho}+\bar{\rho}^2/2+\bar{\mathcal{V}}/3+\bar{\mathcal{N}})+\bar{\mathcal{M}}}{1-6\bar{\mathcal{M}}/x}\right) \times(2\bar{\mathcal{V}}+3\bar{\mathcal{N}}) - \frac{9}{x}\bar{\mathcal{N}} - 3(\bar{p}+\bar{p})\bar{\rho}'. \tag{12c}$$

In contrast to the TOV equations of GR in (10), we shall call this case the high energy limit because the mean density is much larger than the brane tension, even if we cannot say whether this is because the brane tension attains a very small energy value, or it is just that the star has such a large density that the latter surpasses the energy scale of the brane tension.

C. Boundary conditions

The change of variables (7) is very appropriate to explore the solutions of the TOV equations (8), as all physical quantities involved are normalized in terms of two important observables in stellar astrophysics, which are the mass M and the radius R of the star. Furthermore, these two parameters appear in the single combination $G_N M/R$ that represents the compactness of the star. For instance, the interior range of the new radial variable is $x=[0,\sqrt{G_N M/R}]$, which means that the surface of the

star is located at $x(R) \equiv X = \sqrt{G_N M/R}$. Also, the new mass function changes to

$$\bar{\mathcal{M}}(x) = \frac{1}{3}\left(\frac{G_N M}{R}\right)^{3/2}\frac{\mathcal{M}(r)}{M}, \tag{13}$$

and then the total mass is $\bar{\mathcal{M}}(X) = (1/3)(G_N M/R)^{3/2}$. In other words, the compactness of the star will determine the mass and size of the numerical solutions.

The equations of motion will be integrated from the center up to the surface of the star defined by the condition $p(X) = 0$; the latter only refers to the physical pressure, and we will take it as a reasonable physical assumption even though it is not necessarily required in the case of brane stars. Finally, at the center of the star we will also assume that $\bar{\mathcal{M}} \to 0$ as $x \to 0$, so that there is not a discontinuity of the different quantities in the center of the star, and the central value of the pressure (or any other related quantity) will be set as a free parameter that will characterize the numerical solutions.

Even though we will not consider exterior solutions, we must anyway take into account the information provided by the Israel-Darmois (ID) matching condition, which for the case under study can be written as [9]

$$(3/2)\bar{\rho}^2(X) + \bar{\mathcal{V}}^-(X) + 3\bar{\mathcal{N}}^-(X) = \bar{\mathcal{V}}^+(X) + 3\bar{\mathcal{N}}^+(X), \tag{14}$$

where the superscript $-(+)$ denotes the interior (exterior) values of the different quantities at the surface of the star, and we also assumed that $\bar{\rho}(x > X) = 0$.

A desirable property we want in our solutions is a *Schwarzschild exterior*, which can be easily accomplished under the boundary conditions $\bar{\mathcal{V}}^+(X) = 0 = \bar{\mathcal{N}}^+(X)$, as for them the simplest solution that arises from Eq. (8c) is the trivial one: $\bar{\mathcal{V}}(x \geq X) = 0 = \bar{\mathcal{N}}(x \geq X)$. Thus, for the purposes of this paper, we will refer hereafter to the restricted ID matching condition given by

$$(3/2)\bar{\rho}^2(X) + \bar{\mathcal{V}}^-(X) + 3\bar{\mathcal{N}}^-(X) = 0. \tag{15}$$

For completeness, we just note that the exterior solutions of the metric functions are given by the well-known expressions $B(r) = A^{-1}(r) = 1 - 2G_N M/r$. In addition, it can be shown from Eq. (5d) that the interior solution of the lapse function, in terms of the normalized variables (7), is given by

$$\frac{B(x)}{1 - 2G_N M/R} = \exp\left[-\int_x^X dx \frac{6}{x^2}\left(\frac{x^3\bar{p}_{\text{eff}} + \bar{\mathcal{M}}}{1 - 6\bar{\mathcal{M}}/x}\right)\right], \tag{16}$$

and then we will not solve it explicitly in any of the cases presented below.

The numerical recipe described above will be applied to different cases and configurations in Secs. III and IV. The results that will be obtained will have a universal character, as they will not depend upon the particular values of the mass and radius of a given star, but they will represent general classes of stars according to their common compactness $G_N M/R$. This will allow us to reach wide general conclusions about the physical properties of the different configurations by means of numerical methods.

D. Weyl functions

It must be noticed that the interior solutions cannot evade the presence of the Weyl terms even if the exterior solution is Schwarzschild. For example, let us put by hand that $\bar{\mathcal{N}}(x) \equiv 0$. If the density is constant $\bar{\rho}(X) \neq 0$, the ID matching condition (15) implies that $\bar{\mathcal{V}}^-(X) = -(3/2)\bar{\rho}^2(X)$, and then the full solution must be [9]

$$\mathcal{V}(x < X) = -(3/2)\rho^2(1 + p/\rho)^4. \tag{17}$$

The full consequences of this nonlocal energy density $\mathcal{V}$ are explored in Sec. III B below.

Even the condition of a Schwarzschild exterior together with $\bar{\rho}(X) = 0$ does not directly imply that the Weyl functions must vanish in the interior, as it can be shown [12] that in such a case Eq. (8c) must have the following solution:

$$\mathcal{V}(x < X) = \frac{3}{B^2(x)}\int_x^X B^2(\bar{\rho} + \bar{p})\bar{\rho}' dx, \tag{18}$$

which accomplishes the boundary condition $\mathcal{V}^-(X) = 0$ and is also regular at $x = 0$. This is particularly important for all cases in which the density is not constant, as we shall see below for the polytropes in Sec. IV.

In the opposite case when $\bar{\mathcal{V}}(x) \equiv 0$ and the density is constant, the ID matching condition (15) implies that at the surface of the star, $\bar{\mathcal{N}}^-(X) = -(1/2)\bar{\rho}^2(X)$, and then Eq. (8c) integrates into

$$\mathcal{N}(x < X) = -\frac{1}{2}\left(\frac{X}{x}\right)^3(p + \rho)^2. \tag{19}$$

Needless to say, this solution diverges at the center of the star and cannot be considered as a useful interior solution. That is, in the case of constant density there is not a regular interior solution with the only presence of the nonlocal anisotropic stress $\mathcal{N}$.

There is though a nondivergent interior solution of $\mathcal{N}$ if we drop the condition of constant density, which is

$$\mathcal{N}(x < X) = \frac{1}{B(x)x^3}\int_0^x Bx^3(\bar{\rho} + \bar{p})\bar{\rho}' dx. \tag{20}$$

But the ID matching condition (15) now indicates that at the surface of the star we must have $\bar{\rho}(X) \neq 0$, or either give up the Schwarzschild exterior. In consequence, the only interior solution of the nonlocal anisotropic stress under the conditions of a Schwarzschild exterior, and nonconstant density with $\bar{\rho}(X) = 0$, which are the conditions we expect to have in realistic stars, is the trivial one: $\mathcal{N}(x) \equiv 0$ (see also [12]).

There are other possibilities that have been explored in the specialized literature, like for instance a relationship between the Weyl functions in the form $\mathcal{N} = \sigma\mathcal{V}$, where σ is a constant parameter [10]. Clearly, the solutions (17) and (18) are special cases for which $\sigma = 0$. In the general case, Eq. (8c) can be written as

$$(1+3\sigma)\bar{\mathcal{V}}' = -\frac{B'}{B}(2+3\sigma)\bar{\mathcal{V}} - \frac{9}{x}\sigma\bar{\mathcal{V}} - 3(\bar{\rho}+\bar{p})\bar{\rho}', \qquad (21)$$

as long as $\sigma \neq -1/3$. If the density is constant, then there is a solution which is similar to Eq. (19):

$$\bar{\mathcal{V}} = C[(p+\rho)^{2(2+3\sigma)}x^{-9\sigma}]^{1/(1+3\sigma)}, \qquad (22)$$

where C is an integration constant that could be determined with the help of the ID matching condition (15). However, this solution is not appropriate for the interior of the star because, as it happened too for Eq. (19), it diverges in the center of the star ($x = 0$).

We can also consider the case of nonconstant density, in which case we find a similar solution to Eq. (20):

$$\mathcal{N}(x<X) = [B(x)^{-2(2+3\sigma)}x^{-9\sigma}]^{1/(1+3\sigma)} \times \int_0^x [B^{2(2+3\sigma)}x^{9\sigma}]^{1/(1+3\sigma)}(\bar{\rho}+\bar{p})\bar{\rho}'dx. \qquad (23)$$

Even though this solution is well behaved in the interior of the star, it needs a nontrivial boundary condition at the surface as dictated by the ID matching condition (15), and for that we require either to have $\bar{\rho}(X) \neq 0$, or to give up the Schwarzschild exterior.

We see that the imposition of a Schwarzschild exterior has strong consequences for the interior solutions of the Weyl functions, mostly because it is difficult in general to find for them a well-behaved interior solution. The most problematic case is that of the anisotropic stress function $\mathcal{N}$, and for this reason we will not take it into account as part of the brane gravitational corrections, but assume that the latter are only given by the quadratic corrections of the density $\bar{\rho}^2$ and the nonlocal energy density $\mathcal{V}$.

III. THE CASE OF CONSTANT DENSITY

One of the simplest possibilities of star models is that of constant density ρ, which can be solved under different gravitational schemes. In this section we will work out such a case within the brane-world scheme and explain the additional physical and boundary conditions that may be needed in order to reach well-posed numerical solutions.

A. The case of the Germani-Maartens solution of brane stars

To start with we consider here the GM interior solution, which was thoroughly studied in [9], and that does not take into account corrections induced by the Weyl terms: $\bar{\mathcal{V}} = 0 = \bar{\mathcal{N}}$. The modified TOV equations are given again by Eqs. (5a) and (5b) with the following identifications: $\rho_{\rm eff} = \rho(1+\rho/2\lambda)$, and $p_{\rm eff} = p(1+\rho/\lambda) + \rho^2/2\lambda$.

Because the density is constant, we find, in terms of the variables in (7), that $\langle\rho_{\rm eff}\rangle = \rho(1+\rho/2\lambda)$ and then $\bar{\rho}_{\rm eff} = 1$. Likewise, we find that $\bar{\rho} = (1+\rho/2\lambda)^{-1}$, and then its value is directly determined by the ratio ρ/λ. Notice that $\bar{\rho} \leq 1$, and that we recover $\bar{\rho} = 1$ in the GR limit $\rho/\lambda \to 0$. The boundary conditions depend upon the compactness of the star $G_N M/R$, as in the case of GR, but also upon the ratio ρ/λ, as expected in brane models. The exact solution of the pressure function is [9]

$$\frac{\bar{p}}{\bar{\rho}} = \frac{\sqrt{1-6\bar{\mathcal{M}}/X} - \sqrt{1-6\bar{\mathcal{M}}x^2/X^3}}{\sqrt{1-6\bar{\mathcal{M}}x^2/X^3} - 3\zeta^{-1}\sqrt{1-6\bar{\mathcal{M}}/X}}, \qquad (24)$$

where $\zeta \equiv (1+2\rho/\lambda)/(1+\rho/\lambda)$. The brane ratio ρ/λ lowers the maximum value of the compactness of the star, and the numerical solutions satisfies the analytic bound found from the exact GM solution: $G_N M/R = (1/2)(1-\zeta^2/9)$. The GR limit is obtained when $\rho/\lambda \to 0$: $G_N M/R \leq 4/9$, whereas in the opposite direction $\rho/\lambda \to \infty$ we obtain $G_N M/R \leq 5/18$.

According to the discussion in Sec. II D, the GM solution cannot be matched to a Schwarzschild exterior, and for that reason it is usually assumed that other exterior solutions with the presence of the Weyl function must be the correct ones for brane stars. However, it has been recently shown [12], under very general conditions, that the GM solution plays also the role of being the limiting case of realistic stars when brane corrections are considered, and then gives an upper bound in the compactness of stars with both brane corrections and a Schwarzschild exterior.

B. The extended GM solution

We will now review the interior brane solution with constant density, a Schwarzschild exterior, and a non-null Weyl term $\mathcal{V}$. This cases was also briefly considered in [9], but lacks an analytical solution. The equations of motion are again (8) with the following expressions for the effective density and pressure:

$$\bar{\rho}_{\rm eff} = \bar{\rho}\left(1+\frac{\rho}{2\lambda}\right) - \frac{3}{2}\bar{\rho}\frac{\rho}{\lambda}(1+\bar{p}/\bar{\rho})^4, \qquad (25a)$$

$$\bar{p}_{\rm eff} = \bar{p}\left(1+\frac{\rho}{\lambda}\right) + \frac{\bar{\rho}}{2}\frac{\rho}{\lambda} - \frac{\bar{\rho}}{2}\frac{\rho}{\lambda}(1+\bar{p}/\bar{\rho})^4. \qquad (25b)$$

Here we have taken into account that the nonlocal energy density is given by Eq. (17). As it can be seen in Eq. (25), there are negative contributions in both the effective density and pressure that originated from the presence of the Weyl nonlocal energy, and the solutions now depend upon three separate parameters: the constant density ρ, the brane ratio ρ/λ, and the compactness of the star $G_N M/R$.

As we expect to have $p(x) > 0$, then the effective density must be an increasing function, $\rho_{\rm eff}(x) \leq \rho_{\rm eff}(X)$, which may even attain negative values at the interior points where the pressure is largest. Moreover, we also infer from this information that $\langle\rho_{\rm eff}\rangle < \rho_{\rm eff}(X) = \rho(1-\rho/2\lambda)$, and then we expect that, in general, $\bar{\rho} > (1-\rho/2\lambda)^{-1}$. In contrast to the GM case above, $\bar{\rho}$ cannot be given a fixed value beforehand and becomes a variable that must be adjusted appropriately so that the numerical solutions accomplish all boundary conditions. This time, however, the GR limit $\bar{\rho} = 1$ is a lower bound as $\rho/\lambda \to 0$, which is an early indication that the known GR upper bound on the star compactness could, in principle, be surpassed by the new solutions.

The equations of motion are more easily solved if we take the following change of variables:

$$x \to x\bar{\rho}^{-1/2}, \qquad \bar{\mathcal{M}} \to \bar{\mathcal{M}}\bar{\rho}^{-1/2}, \qquad w \equiv p/\rho, \qquad (26)$$

where w is the EOS, and then the Eq. (8) becomes

$$\bar{\mathcal{M}}' = x^2\left[1+\frac{\rho}{2\lambda} - \frac{3}{2}\frac{\rho}{\lambda}(1+w)^4\right], \qquad (27a)$$

$$w' = -\frac{3}{x^2}\left(\frac{x^3 w_{\rm eff} + \bar{\mathcal{M}}}{1-6\bar{\mathcal{M}}/x}\right)(1+w),$$

$$w_{\rm eff} = \frac{\bar{p}_{\rm eff}}{\bar{\rho}} = w\left(1+\frac{\rho}{\lambda}\right) + \frac{\rho}{2\lambda}[1-(1+w)^4]. \qquad (27b)$$

The only free parameter that appears explicitly in Eq. (27) is the brane ratio ρ/λ. Moreover, the outer boundary conditions, see for instance Eq. (13), must be adjusted to the values $X = (G_N M/R)^{1/2}\bar{\rho}^{1/2}$ and $\bar{\mathcal{M}}(X) = (G_N M/R)^{3/2}\bar{\rho}^{1/2}/3$.

Examples of the numerical solutions allowed by Eq. (27) are shown in Fig. 1 for the brane ratios $\rho/\lambda = 10^{-1}, 10^{-6}$, where it is confirmed that there are numerical solutions well beyond the GR limit of $G_N M/R \leq 4/9$. We only considered cases in which the star has an overall positive mass, for which it must also have a positive density at its surface. The latter can be translated into the condition $\bar{\rho}_{\rm eff}(X) > 0$, and then from Eq. (25a) we find the constraint $\rho/\lambda < 1$.

There are two main reasons for the surpass of the GR limit. The first one is that the extra free parameter $\bar{\rho}$ is only bounded from below, and then it is at our disposal to find numerical solutions that can surpass the GR limit for any given value of the brane ratio ρ/λ. Correspondingly, the second reason is that the effective density $\bar{\rho}_{\rm eff}$ is an increasing function that can become as negative as necessary in the interior of the star. Actually, as far as the numerical experiments are concerned, the only true limit that could be found for the numerical solutions is the Schwarzschild one, $G_N M/R < 1/2$.

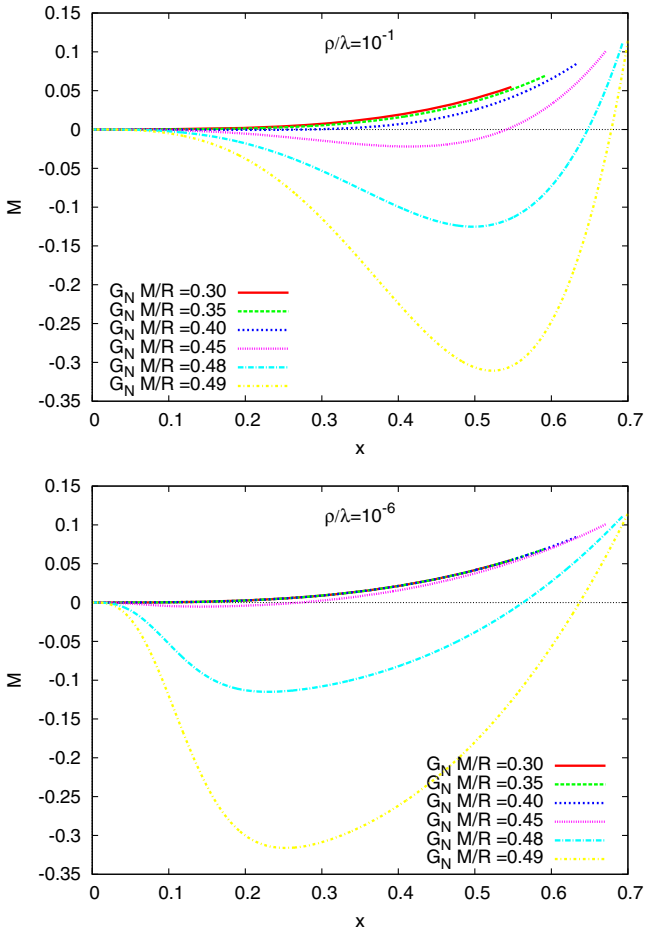

FIG. 1 (color online). The profile of the integrated mass $\mathcal{M}(x)$ corresponding to the extended GM solution with ratios $\rho/\lambda = 10^{-1}$ (top) and $\rho/\lambda = 10^{-6}$ (bottom). We can see that the extended GM solution allows the existence of stars with a compactness beyond the GR limit but below the extreme Schwarzschild limit $G_N M/R < 1/2$. Notice that one reason for that is that the mass function can acquire negative values in the interior of the star for the most compact cases. See the text for more details.

IV. POLYTROPIC BRANE STARS

In this section we study brane stars with a polytropic fluid and an EOS in the form $p(r) = K\rho^\gamma(r)$. Here, K is the polytropic constant, and γ is the polytropic exponent, which can be written in terms of the polytropic index n as $\gamma \equiv (n+1)/n$. For example, white dwarfs can be modeled

by the polytropic index $n = 3$, and neutron stars by polytropes with an index in the range $n = 0.5$–1 [19].

The equations of motion (8) can be simplified if we follow the usual recipe for polytropes and make the following change of variable for the density: $\bar{\rho} = \theta^n$, where n is the polytropic index defined above. For the reasons explained in Sec. II D, we set $\bar{\mathcal{N}} = 0$. Equation (8) is then written in the form

$$\bar{\mathcal{M}}' = x^2\left[\theta^n\left(1+\frac{\theta^n}{2\bar{\lambda}}\right)+\frac{\bar{\mathcal{V}}}{\bar{\lambda}}\right], \tag{28a}$$

$$\theta' = -\frac{3}{x^2}\left(\frac{x^3\bar{p}_{\rm eff}+\bar{\mathcal{M}}}{1-6\bar{\mathcal{M}}/x}\right)\frac{(1+\bar{K}\theta)}{\bar{K}(n+1)}, \tag{28b}$$

$$\bar{\mathcal{V}}' = -\frac{12}{x^2}\left(\frac{x^3\bar{p}_{\rm eff}+\bar{\mathcal{M}}}{1-6\bar{\mathcal{M}}/x}\right)\bar{\mathcal{V}} + \frac{9}{x^2}\left(\frac{x^3\bar{p}_{\rm eff}+\bar{\mathcal{M}}}{1-6\bar{\mathcal{M}}/x}\right)\frac{n(1+\bar{K}\theta)^2}{\bar{K}(n+1)}\theta^{2n-1}, \tag{28c}$$

where $\bar{K} = K\langle\rho_{\rm eff}\rangle^{4/n}$ and the effective pressure (9b) now reads

$$\bar{p}_{\rm eff} = \bar{K}\theta^{n+1}\left(1+\frac{\theta^n}{\bar{\lambda}}\right)+\frac{\theta^{2n}}{2\bar{\lambda}}+\frac{\bar{\mathcal{V}}}{3\bar{\lambda}}. \tag{29}$$

It must be stressed that in our case the density parameter θ gives an indication of the values of the density ρ with respect to the mean value of the effective density $\langle\rho_{\rm eff}\rangle$, given by the dimensionless density $\bar{\rho}$, in contrast to the standard case in which the value of reference is the density at the center of the star $\rho(0)$.

It can also be shown that, again like in the standard case of polytropes, the polytropic coefficient $\bar{K}$ is a redundant constant and can be hidden in the equations of motion. If we further consider the following change of variables:

$$x \to x\bar{K}^{n/2}, \qquad \theta \to \theta\bar{K}^{-1}, \qquad \bar{\mathcal{M}} \to \bar{\mathcal{M}}\bar{K}^{n/2}, \tag{30a}$$

$$\bar{p}_{\rm eff} \to \bar{p}_{\rm eff}K^{-n}, \qquad \bar{\lambda} \to \bar{\lambda}\bar{K}^{-n}, \qquad \bar{\mathcal{V}} \to \bar{\mathcal{V}}\bar{K}^{-2n}, \tag{30b}$$

then Eq. (28) simply reads

$$\bar{\mathcal{M}}' = x^2\left[\theta^n\left(1+\frac{\theta^n}{2\bar{\lambda}}\right)+\frac{\bar{\mathcal{V}}}{\bar{\lambda}}\right], \tag{31a}$$

$$\theta' = -\frac{3}{x^2}\left(\frac{x^3\bar{p}_{\rm eff}+\bar{\mathcal{M}}}{1-6\bar{\mathcal{M}}/x}\right)\frac{(1+\theta)}{(n+1)}, \tag{31b}$$

$$\bar{\mathcal{V}}' = -\frac{12}{x^2}\left(\frac{x^3\bar{p}_{\rm eff}+\bar{\mathcal{M}}}{1-6\bar{\mathcal{M}}/x}\right)\bar{\mathcal{V}} + \frac{9}{x^2}\left(\frac{x^3\bar{p}_{\rm eff}+\bar{\mathcal{M}}}{1-6\bar{\mathcal{M}}/x}\right)\frac{n(1+\theta)^2}{(n+1)}\theta^{2n-1}, \tag{31c}$$

where

$$\bar{p}_{\rm eff} = \theta^{n+1}\left(1+\frac{\theta^n}{\bar{\lambda}}\right)+\frac{\theta^{2n}}{2\bar{\lambda}}+\frac{\bar{\mathcal{V}}}{3\bar{\lambda}}. \tag{32}$$

Our main interest is the numerical solutions of stars with a finite size, as determined by the boundary condition $p(X) = 0$, which in the case of the polytropes translates into $\rho(X) = 0$, and from this into $\theta(X) = 0$. In order to avoid any singularities in the equations of motion at the surface of the star, in particular for Eq. (31c), we must constrain the values of the polytropic index in the range $n \geq 1/2$. Needless to say, such a constraint does not exist either in the case of nonrelativistic (Newtonian) or relativistic (GR) polytropes. It must be noticed as well that the boundary conditions should also be adjusted so that $X = (G_N M/R)^{1/2}\bar{K}^{-n/2}$ and $\bar{\mathcal{M}}(X) = (1/3)(G_N M/R)^{3/2}\bar{K}^{-n/2}$.

We now include brane corrections with the contribution of one of the Weyl terms, with the boundary condition $\bar{\mathcal{V}}(X) = 0$, so that the ID matching condition (14) allows a Schwarzschild exterior for the polytrope and dictates that the interior solution for the nonlocal energy density is given by Eq. (18). As discussed in Sec. II B, the brane terms must contribute to the effective density and pressure inside the star, which means that we cannot have, in this case, a counterpart of the GM solution, unless the Schwarzschild condition was waived.

As in the cases studied in Sec. III, we will integrate inwards the equations of motion under the same boundary conditions presented in Sec. II C, with the central value of $\theta(0)$ being a free parameter that will help us to classify the numerical solutions. The most compact star will be given by the maximum in the plot of the compactness as a

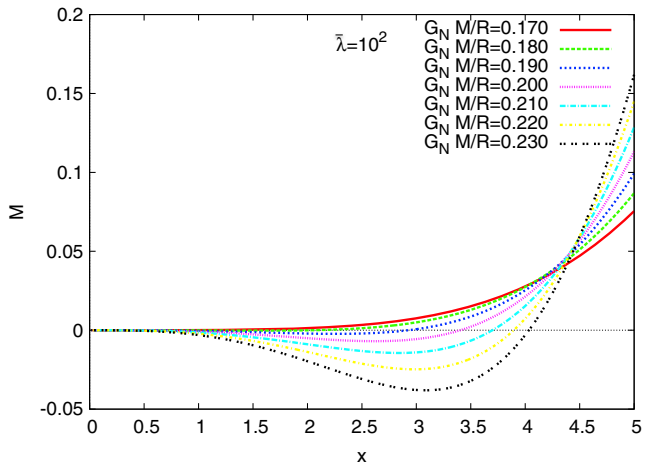

FIG. 2 (color online). Numerical solutions of the interior profile of the mass M of polytropic brane stars, see Eq. (31), with $\bar{\lambda} = 10^2$. We can observe for $G_N M/R \geq 0.180$ that the mass becomes negative, like in the constant density case shown in Fig. 1. This is due to the contribution of the Weyl function $\bar{\mathcal{V}}$; see text for more details.

function of the central density: $G_N M/R$ vs $\theta(0)$. The value of the compactness will be read off from the outermost points of the numerical solution as $G_N M/R = 3\bar{\mathcal{M}}(X)/X$, whereas the polytropic coefficient can be calculated from $\bar{K} = [3\bar{\mathcal{M}}(X)/X]^{1/n}$.

This time we have to give explicit values to the brane tension $\bar{\lambda}$ and the polytropic index n. For the latter, we consider in the following sections the case of white dwarfs with $n = 3$, whereas the brane tension will remain free to label the different brane star solutions.

A. Numerical solutions

Solutions for the high energy limit with $\bar{\lambda} = 10^2$ allowed by Eq. (31) are shown in Figs. 2 and 3. In particular, the interior mass profile $M(x)$ is shown in Fig. 2 for a range of compactness: $G_N M/R = 0.170$–0.230, in which the main feature we can observe is a change in sign close to the center of the star for $G_N M/R \geq 0.180$. This behavior is due to the contribution of the Weyl function $\bar{\mathcal{V}}$ in Eq. (31a). Note that the same behavior occurs in the constant density case in Sec. III B, so this type of effect from the Weyl function is present also in more realistic stars.

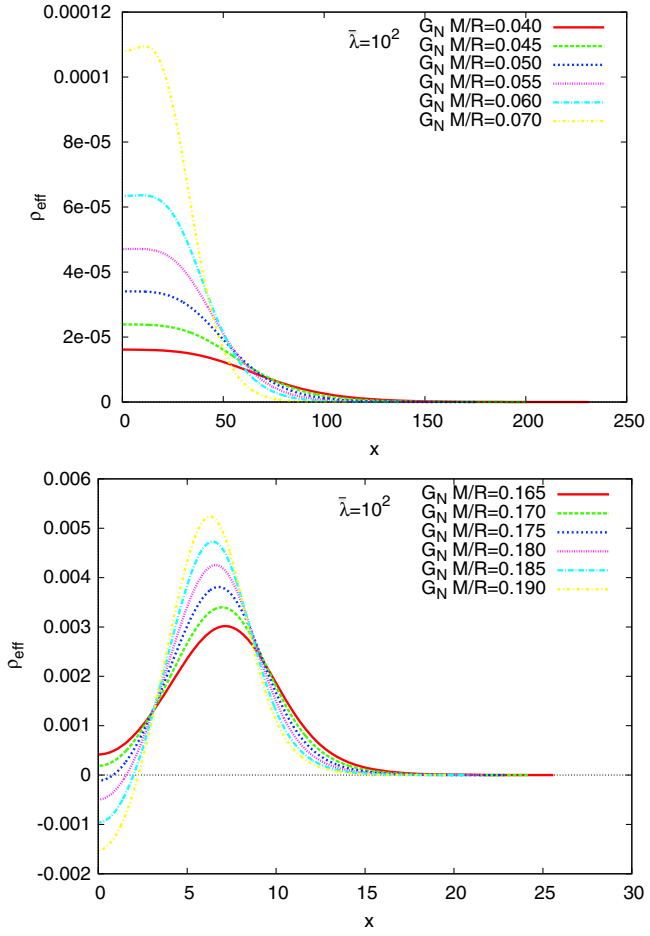

FIG. 3 (color online). (Top) The effective energy density $\bar{\rho}_{\rm eff}$ as a function of the radial coordinate x, which results from the numerical solution of Eq. (31) for low compactness and $\bar{\lambda} = 10^2$. It can be seen that, as the compactness increases, the maximum of the effective density is displaced from the center of the star. (Bottom) The interior profiles of the effective density $\bar{\rho}_{\rm eff}$ for high compactness. The effect of the Weyl term $\bar{\mathcal{V}}$ is sufficiently large to change the sign of the effective density at the center; actually, $\bar{\rho}_{\rm eff}(x = 0) < 0$ for $G_N M/R \geq 0.175$.

On the other hand, numerical solutions with $\bar{\lambda} = 10^2$ in Fig. 3 show that for low compactness the effective density has the expected decreasing behavior as we move outwards from the center of the star. However, as the compactness increases the maximum value of the density is displaced from the center, and then the density profile is not just a decreasing function. Also note that the effective density at the center becomes negative for $G_N M/R \geq 0.175$. It is clear that the geometric term $\bar{\mathcal{V}}$ contributes notoriously for large values of the compactness in the high energy limit.

Thus, at least for the range of compactness we numerically explored, the contribution of the Weyl tensor affects the internal configurations of the stars in such a way that there is no maximum for the compactness that can be reached, except for the Schwarzschild bound $G_N M/R < 0.5$. This can be seen in Fig. 4, where we show the compactness $G_N M/R$ of the solutions as a function of the central value $\theta(0)$ as defined in Eq. (28). As expected, for the cases $\bar{\lambda} = 10^6, 10^5$ the curves reach a value of maximum compactness just as in the case of polytropic stars in GR.

However, as the value of $\bar{\lambda}$ decreases it is possible to see two anomalous features of the curves. First, they do not show a maximum of the compactness for $\bar{\lambda} < 10^4$, but rather suggest the existence of stellar configurations with a compactness beyond the standard GR bound. Second, it is not possible to find solutions beyond certain values of $\theta(0)$,

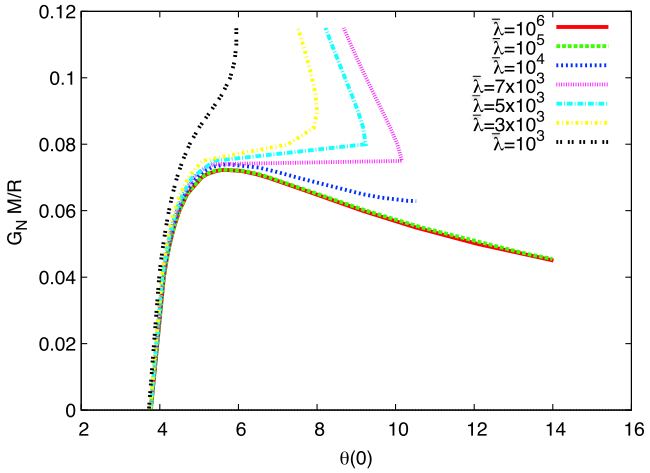

FIG. 4 (color online). The compactness $G_N M/R$ as a function of the central value $\theta(0)$ for the polytropic configurations obtained from Eq. (31). It can be seen that the compactness of the polytropic star with $n = 3$ is not bounded as $\bar{\lambda} \to 0$. For $\bar{\lambda} = 10^6, 10^5$ the curves coincide with that of polytropes in GR.

TABLE I. Mass M and radius R, in solar units $M_\odot$ and $R_\odot$, respectively, of several white dwarfs as reported in [20], where the last column indicates the mean density $\langle\rho_{\rm eff}\rangle = 3M/4\pi R^3$. Note that CD below refers to the Córdova-Durchmusterung star catalog. See the text for more details.

White Dwarf	Mass ($M_\odot$)	Radius ($R_\odot$)	$\langle\rho_{\rm eff}\rangle$ (MeV^4)
Sirius B	1.034	0.0084	10.5993
Procyon B	0.604	0.0096	4.1478
40 Eri B	0.501	0.0136	1.21009
EG 50	0.50	0.0104	2.70063
GD 140	0.79	0.0085	7.81565
CD-38 10980	0.74	0.01245	2.3298
W485A	0.59	0.0150	1.06212

which suggest that the central value of the effective density $\rho_{\rm eff}(0)$ must decrease for large values of the compactness. This is also shown, for example, in Fig. 3, where we can observe that $\rho(0)$ is not always the maximum value of the effective density inside the star. For such configurations, the contribution of the Weyl term $\mathcal{V}$ to the effective density becomes important for small values of the brane tension, in a similar manner as for the extended GM case studied in Sec. III B.

The curves in Fig. 4 represent families of equilibrium configurations that share the same value of $\bar{\lambda} = \lambda/\langle\rho_{\rm eff}\rangle$, and this suggests that we can use real dwarf stars as gravitational laboratories to constrain the value of the brane tension λ. We show in Table I the measured values of the mass M and radius R of several white dwarfs as reported in the recent literature [20], which we use in order to calculate their mean density $\langle\rho\rangle = 3M/4\pi R^3$ in units of MeV^4. We must recall that one of our main assumptions is that the mean density in our numerical solutions takes into account the brane corrections; see Sec. II A. Thus, if we now consider that the white dwarfs in Table I should belong to any of the theoretical curves in Fig. 4 without an anomalous behavior, we can conclude that $\bar{\lambda} > 10^4$. This can be translated into the lower bound $\lambda > 10^4$ MeV^4, which is consistent with other constraints estimated from astrophysics and cosmology [5,6].

V. CONCLUSIONS AND REMARKS

In this paper we studied the equilibrium configurations of stars with gravitational corrections in brane-world models, and provided numerical solutions when necessary. For that we considered the high and low energy limits of the equations of motion to show the threshold between GR and brane worlds, and explored the appropriate boundary conditions to obtain general conclusions about the physical properties of the different stellar configurations.

Our analysis took into account the corresponding Weyl functions which provide nonlocal terms in the pressure and density, and which can have noticeable effects in diverse features of a star. This study allows us to relinquish the nonlocal anisotropic stress under the conditions of a Schwarzschild exterior and nonconstant density, which are conditions rightly expected for a real star.

As an initial test, we revisited the case of constant density, corresponding to the GM solution, but later studied the so-called *extended* GM solution, for which stars exist with a compactness beyond the standard GR bound. This is due mainly to the existence of the nonlocal terms which provoke the appearance of negative values of the effective density and mass in the interior of the star.

We then considered the case of a white dwarf star modeled with a polytropic EOS and index $n = 3$. In similarity with the extended GM case, our results proved the existence of dwarf stars with a compactness beyond the GR limit, because of the presence of nonlocal terms. Also, the compactness of dwarf stars is not bounded as the brane tension tends to zero, which corresponds to the high energy limit, while in the low energy limit we recovered the classical compactness reported in the literature for the case of GR. All these results are in agreement with the study in [12], where it was shown that one of the main requirements for the existence of an upper bound in the compactness of a star is that the effective energy density in the interior should be a decreasing function. Finally, under the assumption that observed white dwarfs must belong to a family of equilibrium configurations without an anomalous behavior, we were able to suggest a lower bound for the brane tension that is in agreement with other constraints reported previously.

The results presented were based on a clear methodology that makes the equations of motion of brane worlds more tractable in numerical terms that in other analyses in the literature. As noted, the presence of brane corrections modifies in a notorious way the compactness, mass, and other physical characteristics in stellar dynamics, even under the assumption of a Schwarzschild exterior. Extended studies along the lines suggested in this paper can be used to constrain the value of the brane tension using observational data provided by stellar dynamics, and with that to find evidence for the presence of extra dimensions. As a final note, we cannot say if all the configurations found would be gravitationally stable, but it is very likely that those with a negative effective density in the interior may not be able to prevent the collapse into configurations well within the general bound found in [12]. This is work in progress that will be reported elsewhere.

ACKNOWLEDGMENTS

M. A. G.-A. acknowledges support from Cátedra-CONACYT and SNI, and also thanks the Departamento de Física of the University of Guanajuato for its kind hospitality in a postdoctoral stay. L. A. U.-L. wishes to thank Andrew Liddle and the Royal Observatory,

Edinburgh, for their kind hospitality in a fruitful sabbatical stay. This work was partially supported by PROMEP, DAIP-UG (534/2015), PIFI, and by CONACyT México under Grants No. 232893 (sabbatical), No. 167335, and No. 179881. We also thank the support of the Fundación Marcos Moshinsky, the Instituto Avanzado de Cosmología (IAC), and the Beyond Standard Theory Group (BeST) Collaborations.

[1] S. Chandrasekhar, *The Mathematical Theory of Black Holes* (Oxford University Press, New York, 1983); R. C. Tolman, *Relativity, Thermodynamics, and Cosmology* (Dover, New York, 1987); J. R. Oppenheimer and G. M. Volkoff, Phys. Rev. **55**, 374 (1939).

[2] S. Chandrasekhar, *An Introduction to the Study of Stellar Structure* (Dover, New York, 1958), Vol 2; S. Weinberg, *Gravitation and Cosmology: Principles and Applications of the General Theory of Relativity* (Wiley, New York, 1972), Vol 1.

[3] A. Mukherjee, S. Shah, and S. Bose, Phys. Rev. D **91**, 084051 (2015); S. Valdez-Alvarado, C. Palenzuela, D. Alic, and L. A. Ureña López, Phys. Rev. D **87**, 084040 (2013); P.-H. Chavanis and T. Harko, Phys. Rev. D **86**, 064011 (2012).

[4] J. Chagoya, K. Koyama, G. Niz, and G. Tasinato, J. Cosmol. Astropart. Phys. 10 (2014) 055.

[5] A. Perez-Lorenzana, J. Phys. Conf. Ser. **18**, 224 (2005).

[6] R. Maartens and K. Koyama, Living Rev. Relativity **13**, 5 (2010).

[7] L. Randall and R. Sundrum, Phys. Rev. Lett. **83**, 3370 (1999); **83**, 4690 (1999).

[8] T. Shiromizu, K. Maeda, and M. Sasaki, Phys. Rev. D **62**, 024012 (2000).

[9] C. Germani and R. Maartens, Phys. Rev. D **64**, 124010 (2001).

[10] L. B. Castro, M. D. Alloy, and D. P. Menezes, J. Cosmol. Astropart. Phys. 08 (2014) 047.

[11] J. Ovalle, F. Linares, A. Pasqua, and A. Sotomayor, Classical Quantum Gravity **30**, 175019 (2013); J. Ovalle and F. Linares, Phys. Rev. D **88**, 104026 (2013); J. Ovalle, L. Á. Gergely, and R. Casadio, Classical Quantum Gravity **32**, 045015 (2015); R. Casadio, J. Ovalle, and R. da Rocha, arXiv:1503.02873.

[12] M. A. García-Aspeitia and L. A. Ureña Lopez, Classical Quantum Gravity **32**, 025014 (2015).

[13] M. A. Garcia-Aspeitia, M. J. Reyes-Ibarra, C. Ortiz, J. Lopez-Dominguez, and S. Hinojosa-Ruiz, arXiv:1412.3496.

[14] D. Kapner, T. Cook, E. Adelberger, J. Gundlach, B. R. Heckel *et al.*, Phys. Rev. Lett. **98**, 021101 (2007); S. Alexeyev, K. Rannu, P. Dyadina, B. Latosh, and S. Turyshev, JETP **147**, 1120 (215).

[15] J. Sakstein, B. Jain, and V. Vikram, Int. J. Mod. Phys. D **23**, 1442002 (2014); M. A. Garca-Aspeitia, Rev. Mex. Fis. **60**, 205 (2014).

[16] H. Kudoh, T. Tanaka, and T. Nakamura, Phys. Rev. D **68**, 024035 (2003); M. Cavaglia, Int. J. Mod. Phys. A **18**, 1843 (2003).

[17] R. Holanda, J. Silva, and F. Dahia, Classical Quantum Gravity **30**, 205003 (2013); J. D. Barrow and R. Maartens, Phys. Lett. B **532**, 153 (2002); P. Brax and C. van de Bruck, Classical Quantum Gravity **20**, R201 (2003).

[18] V. Pavlidou and T. N. Tomaras, J. Cosmol. Astropart. Phys. 09 (2014) 020.

[19] S. Chandrasekhar, Mon. Not. R. Astron. Soc. **95**, 207 (1935).

[20] S. Balberg and S. L. Shapiro, arXiv:astro-ph/0004317; H. L. Shipman, J. Provencal, E. Høg, and P. Thejll, Astrophys. J. Lett. **488**, L43 (1997); J. B. Holberg, M. Barstow, F. Bruhweiler, A. Cruise, and A. Penny, Astrophys. J. **497**, 935 (1998).